Collisions of DCl with Liquid Glycerol: Evidence for Rapid, Near-Interfacial D → H Exchange and Desorption

Bradley R. Ringeisen,† Annabel H. Muenter, and Gilbert M. Nathanson*

Department of Chemistry, University of Wisconsin—Madison, 1101 University Avenue, Madison, Wisconsin 53706-1322

Received: October 25, 2001; In Final Form: January 30, 2002

Molecular beam scattering experiments are used to identify a submicrosecond, near-interfacial DCl → HCl exchange pathway following collisions of DCl with pure and NaOH-doped glycerol. We find that ∼7% of the thermally equilibrated DCl molecules undergo D → H exchange at or just below the surface of glycerol and then desorb immediately as HCl before they enter the bulk liquid. The data are consistent with exchange occurring within a near-interfacial cage of glycerol molecules, either through an ionic or neutral reaction between the DCl molecule and the surrounding OH groups of glycerol. An additional ∼20% of the thermalized DCl molecules desorb immediately before proton exchange can occur, whereas the remaining ∼73% of the DCl molecules dissociate in the interfacial or deeper regions and dissolve as ions within bulk glycerol for long times. The existence of a rapid D → H exchange and desorption pathway demonstrates that reactions between a gaseous acid and a protic solvent can be confined to the near-interfacial region of the solvent even when bulk solvation of the ionized acid is very favorable.

Introduction

This companion paper continues our study of HCl solvation in liquid glycerol. We use modulated molecular beam scattering techniques to identify and characterize the rapid D → H exchange of DCl at or just below the surface of pure and NaOH-doped glycerol. Our objective is to explore how the near-interfacial region of a protic solvent can act as a self-contained reaction medium even when the solute, DCl, readily dissolves as ions in the bulk region of the liquid.

Mechanisms for HCl dissociation in the bulk and interfacial regions of a protic liquid have been investigated most thoroughly in aqueous solutions. Ab initio calculations predict that HCl ionizes when embedded within a cluster of four or more water molecules[1−7] and that in liquid water HCl initially forms a contact-ion pair by passing over a free-energy barrier smaller than *RT*.[8] The formation of the initial $H^+ \cdot Cl^-$ and subsequent $H^+ \cdot H_2O \cdot Cl^-$ ion pairs is guided by the motions of H_2O within the solvent cage. In low-polarity solvents ($\epsilon = 2$ and 13), calculations predict that $HCl \cdot H_2O$ complexes also generate $Cl^- \cdot H_3O^+$ with a barrier less than *RT*, indicating that H^+ readily moves back and forth between the neutral and ionic structures at 300 K even in nonaqueous environments.[9]

Theoretical studies further predict that HCl ionizes when it is embedded within the first bilayer of ice[10,11] and on top of the ice layer if free OH groups are available for coordination.[12] In both cases, formation of two hydrogen bonds between HCl and water molecules enhances the probability for ionization. Infrared spectroscopy[13−17] and ion scattering[18] measurements demonstrate that HCl exists in both molecular and ionic states in the interfacial region of ice, depending on temperature, HCl concentration, and the availability of free OH surface groups.

Recent experiments also provide evidence about the behavior of HCl near the surface of water. Sum frequency measurements were unable to detect molecular HCl in solutions up to 12 M HCl, implying that it exists largely in ionic form in the near-interfacial region.[19−21] Gas uptake studies further show that only 6−10% of thermally impinging HCl molecules penetrate through the interface and dissolve in pure water at 294 K.[22,23] These studies also indicate that impinging ethanol molecules, in addition to dissolving in bulk water or desorbing from the interface, can undergo proton exchange in the near-interfacial region and leave before dissolving in the bulk, a result that parallels our findings below for DCl in glycerol.[24]

Experiments involving sulfuric acid additionally highlight the role of HCl in interfacial reactions. In particular, steady-state kinetics measurements demonstrate that in 50−70 wt % sulfuric acid the reactions of HCl with $ClONO_2$ and with HONO to produce Cl_2 and ClNO occur in distinct interfacial and bulk regions of the acid.[25,26] Our molecular beam studies of HCl collisions with deuterated sulfuric acid show that H → D exchange occurs within 10 μs in 65 wt % D_2SO_4 at 213 K, likely proceeding through dissociation and recombination within the outermost 50 Å of the acid.[27,28] The H → D exchange probabilities rise from 0.1 to 0.8 as the acid is diluted from 70 to 52 wt % D_2SO_4 and more interfacial water becomes available for protonation. The HCl molecules that do not undergo exchange dissolve for less than 10^{-6} s, suggesting that these molecules thermalize in the interfacial region but desorb before they dissociate.

These studies provide motivation for exploring DCl solvation and dissociation in the near-interfacial region of glycerol, $HOCH_2CH(OH)CH_2OH$, a low vapor pressure liquid that readily dissolves acids, bases, and salts.[29] As reported in the preceding paper, HCl dissolves exothermically ($\Delta H_{HCl}^\circ = -67$ kJ mol^{-1}) and favorably in glycerol ($K_{HCl} = 2300$ M^2 atm^{-1} at 294 K for $HCl(g) \rightleftharpoons H^+(gly) + Cl^-(gly)$) and resides on average for 1 to 0.1 s in the bulk for incident HCl fluxes of 2×10^{14} to 2×10^{15} cm^{-2} s^{-1}, respectively. The inverse relation between bulk residence time and incident HCl flux and the observation of

* Corresponding author. E-mail: nathanson@chem.wisc.edu.
† Present address: Naval Research Laboratory, Washington, D.C. 20375.

10.1021/jp013959x CCC: $22.00
Published on Web 04/23/2002

DCl → HCl exchange imply that longtime solvation is accompanied by dissociation into H^+ and Cl^- ions, in accord with the equilibrium expression $K_{HCl} = [H^+][Cl^-]/P_{HCl}$. We use these results below to help identify and characterize a rapid DCl → HCl exchange and desorption pathway that occurs at or just below the surface of glycerol.

Experimental Section

Scattering Studies. We used the same apparatus described in the preceding paper to monitor near-interfacial DCl → HCl exchange in pure and NaOH-doped glycerol. The 75 mL glycerol sample was cooled in the reservoir to $T_{gly} = 273 \pm 2$ K. This cooling lowers the glycerol vapor pressure to 6×10^{-6} Torr and suppresses the background in the time-of-flight (TOF) spectra attributed to dissociative ionization of glycerol at $m/e = 38$, where $H^{37}Cl$ is monitored. Cooling also raises the viscosity of glycerol from 1300 cP at 294 K to 12 100 cP at 273 K. To accommodate the more viscous liquid, the scattering measurements were performed at the lowest rotation speed of the glycerol-covered disk of 0.083 Hz. The glycerol film is 0.25 mm thick at this wheel speed and is exposed to the incident DCl beam for an exposure time t_{exp} of 0.45 s.

The DCl beams are formed by bubbling HCl seeded in H_2, He, or N_2 through a 37 wt % DCl/D_2O solution and expanding the mixture through a 0.07-mm diameter nozzle at 403 K. The resulting beams have energies of 95, 53, and 14 kJ mol^{-1}, respectively. The HCl content in the DCl beams ranges from 5 to 8% and generally rises after 5 h as the DCl solution is depleted of deuterium. The DCl/HCl ratio was determined in each experiment by comparing the inelastic scattering signals at the $D^{37}Cl$ and $H^{37}Cl$ masses. To model the scattering of this HCl contaminant, HCl beams were also created at each energy by bubbling HCl through a 37 wt % HCl/H_2O solution.

Basic Glycerol. Solutions of 0.015 and 0.17 M NaOH in glycerol were prepared by adding aqueous NaOH to pure glycerol and degassing the mixture to remove water. OH^- immediately extracts a proton from glycerol and generates H_2O, which evaporates under vacuum, and $C_3H_7O_3^-$ ions.[30] NMR spectra of the liquid before and after addition of NaOH showed similar trace impurities, indicating that NaOH does not react further with glycerol at these concentrations.

The surface tensions of 0−0.26 M dewatered NaOH/glycerol solutions were measured at 294 K using the Wilhelmy method[31] with a 3.63-cm perimeter Pt plate. The Na^+ and $C_3H_7O_3^-$ ions increase the surface tension of glycerol by roughly 1 dyne cm^{-1} for 0.26 M NaOH, implying that these ions are depleted in the surface region. Repeated measurements yield surface tension increments of 0.8 ± 0.5 (0.10 M NaOH), 1.0 ± 0.2 (0.17 M NaOH), and 1.1 ± 0.4 (0.26 M NaOH) dyne cm^{-1}. These values were analyzed using the Gibbs adsorption equation to determine the depletion of $C_3H_7O_3^-$ in the surface region.[32] The small changes in surface tension lead to large uncertainties in interfacial ion concentrations; at 0.17 M $C_3H_7O_3^-$, the surface deficit of $C_3H_7O_3^-$ is computed to be $(5 \pm 10) \times 10^{12}$ cm^{-2}. This deficit is equal to the expected $C_3H_7O_3^-$ interfacial density of 5.0×10^{12} cm^{-2} for the 0.17 M solution in the absence of surface depletion. If the measured depletion is restricted to the outermost surface layer, then there will be no ions in this layer and the NaOH-doped solution can be described as a monolayer of pure glycerol covering a bulk solution of 0.17 M $C_3H_7O_3^-$ and Na^+ ions. This dilute solution corresponds to 1 $C_3H_7O_3^-$ ion for every 80 glycerol molecules.

Results and Analysis

The DCl and HCl time-of-flight (TOF) spectra in Figures 6 and 7 of the preceding paper demonstrate that DCl molecules colliding into liquid glycerol follow at least three pathways: direct inelastic scattering (IS) of DCl from surface glycerol molecules, trapping and thermal desorption (TD) of DCl before exchange, and trapping and longtime solvation of DCl accompanied by dissociation of DCl and $D^+ \rightarrow H^+$ exchange before the Cl^- and H^+ ions recombine and desorb as HCl. We use modulated beam techniques below to identify an unexpected fourth pathway involving rapid, near-interfacial D → H exchange and desorption.

Residence Times from Pre- and Post-Chopper TOF Spectra. DCl and HCl residence times in glycerol can be measured from less than 10^{-6} s to greater than 10^{-3} s by recording TOF spectra using "post-chopper" and "pre-chopper" wheels to modulate the scattered and incident molecules, respectively.[28] The chopper wheel geometry is shown in Figure 2 of the preceding paper. In the post-chopper configuration, DCl molecules strike the glycerol film continuously, and the exiting DCl and HCl molecules are chopped into 20-μs gas pulses by spinning an 18 cm diameter wheel with four 1.6-mm slots at 150 Hz. The arrival times of the scattered molecules are recorded by a mass spectrometer at incident and exit angles of $\theta_{inc} = \theta_{fin} = 45°$. The post-chopper arrival times are determined by the velocities of the scattered HCl and DCl and are not related to their residence times in the glycerol film. Modulation of the incident DCl beam before the molecules reach the film provides a method to measure the HCl and DCl residence times in solution. These pre-chopper TOF spectra are recorded by chopping the incident DCl beam into 50-μs pulses using a 2.5-cm diameter cylinder with two 1.6 mm slots. In this configuration, the arrival time of an HCl or DCl molecule at the mass spectrometer is the sum of its incident and scattered gas-phase flight times and the time it spends in contact with the glycerol film.

The arrival times of a molecule at the mass spectrometer for the pre- and post-chopper configurations are

$$t_{arrival}(\text{pre-chopper}) = d_{inc}/v_{inc} + t_{res} + d_{pre}/v_{fin} \qquad (1)$$

$$t_{arrival}(\text{post-chopper}) = d_{post}/v_{fin}$$

The distances are depicted in Figure 2 of the preceding paper. For our apparatus, $d_{inc} = 5.0$ cm and $d_{pre} = 24.0$ cm are the distances from the pre-chopper to the glycerol film and from the glycerol to the mass spectrometer, and $d_{post} = 19.3$ cm is the distance from the post-chopper to the mass spectrometer. The incident DCl velocity is v_{inc}, and the velocity of the scattered or desorbed HCl or DCl is v_{fin}. The time t_{res} is the time that the HCl or DCl spends in contact with glycerol before desorbing, which is equal to the sum of the surface and bulk residence times. The method we use to extract t_{res} assumes that the surface residence times are less than 10^{-6} s and thus that any observable differences between the pre- and post-chopper spectra arise primarily from the bulk solvation times of Cl^- and H^+/D^+.

The distribution of bulk residence times is determined by placing the post-chopper spectrum on the pre-chopper time and signal axes, which is achieved by first multiplying $t_{arrival}$(post-chopper) by d_{pre}/d_{post} and by shifting the arrival times and signal levels so that the IS components of each spectrum overlap. These adjustments remove the d_{inc}/v_{inc} offset in eq 1, correct for the different duty cycles of the two chopper wheels, and set the residence time for inelastically scattered molecules to zero, as expected for the picosecond duration of a direct collision. Any

remaining differences in the arrival times and intensities of the pre- and post-chopper spectra are due to the residence times of HCl or DCl in glycerol before they desorb.

The TOF spectra are modeled by assuming that DCl spends most of its time in glycerol as separated Cl^- and D^+/H^+ ions, but our conclusions do not change if it remains in molecular form or as a contact-ion pair (see ref 33). The time and intensity shifts in the TOF spectra are modeled by computing the relative flux or probability, $p_{des}(t)$, that molecules entering glycerol during the 50-μs gas pulse desorb at time t during or after the gas pulse. This probability is given by $p_{des}(t) = F_{des}(t)/F_{des}^* = [c(x = 0, t)/c^*]^2$, where $F_{des}(t)$ is the flux of desorbing HCl, $c(x = 0, t)$ is the concentration of Cl^- at the boundary separating the gas and liquid, and * signifies the value at saturation. The dependence of F_{des} on c^2 arises from the equilibrium expression $K_{HCl}(gly) = c_{H^+}c_{Cl^-}/P_{HCl}$, the equality of c_{H^+} and c_{Cl^-}, and the linear relation between gas flux and gas pressure. The calculation of $p_{des}(t)$ from the diffusion equation is described in the Appendix of the preceding paper.

The $p_{des}(t)$ distributions are characterized by a single variable, the bulk residence or solvation time τ (see eqs 2 and 3 of the preceding paper):[34]

$$\tau = \left(\frac{4D_{HCl}K_{HCl}RT_{gly}}{\beta_{th}\upsilon_{th}F_{in}}\right)\left(\frac{1000}{N_A}\right) \qquad (2)$$

$D_{HCl} = D_{H^+}D_{Cl^-}/(D_{H^+} + D_{Cl^-}) \approx D_{Cl^-}$ is the diffusion coefficient of HCl dissolved in glycerol, β_{th} is the fraction of DCl molecules in an impinging thermal gas (with average velocity υ_{th}) that enter glycerol as either DCl or as Cl^- and D^+/H^+ after dissociation in the interfacial region, and F_{in} is the flux of DCl molecules entering glycerol at E_{inc} and θ_{inc}.[35,36] The characteristic residence time τ is the time required for the flux of desorbing HCl molecules to rise from 0 at $t = 0$ to 48% of its maximum flux as the glycerol becomes saturated with HCl and the net uptake drops toward zero. It is the bulk solvation time τ that is extracted from the pre- and post-chopper comparison. We emphasize that the analysis used to extract τ does not include the surface residence time of the DCl molecule between initial trapping and bulk dissolution or the residence time of the newly formed HCl at the surface before it desorbs. We estimate below that these surface times are less than 10^{-6} s at 273 K.

Graphs of $p_{des}(t)$ for $\tau = 10^{-6}$ to 10^{-1} s are shown in Figure 1a. The beam-on and beam-off regions apply to molecules desorbing during and after the 50-μs gas pulse, respectively. The areas under each curve are equal because the same number of molecules enter the liquid and eventually desorb. The desorption flux initially rises with time as liquid near the surface becomes saturated with gas and then drops after 50 μs because there are no impinging molecules to replenish those that desorb. For $\tau = 0$ s, the desorbing molecules follow the shape of the pre-chopper pulse with zero residence time. As τ increases, the dissolving molecules diffuse deeper into the liquid and desorb over a wider range of times. The peak desorption flux drops slowly with increasing τ, enabling residence times of less than 10^{-6} s to greater than 10^{-3} s to be interrogated with the pre-chopper technique.

The corresponding pre-chopper simulations $N_{sim}(t_{arrival})$ are obtained by convoluting $p_{des}(t)$ with a Maxwell−Boltzmann distribution N_{MB} for HCl at 273 K according to

$$N_{sim}(t_{arrival}) = \int_0^{t_{arrival}} p_{des}(t)N_{MB}(t_{arrival} - t)\,dt$$

The simulated spectra are displayed in Figure 1b as a function of τ; they show that the peak intensities drop and the spectra shift to longer arrival times as τ increases. In particular, the spectra reveal that even characteristic residence times of 10^{-6} s reduce the desorption signal measurably from the $\tau = 0$ s spectrum (which is equal to N_{MB} convoluted with the 50-μs square pulse). This reduction occurs because a small fraction of molecules dissolve deeply into the liquid and do not desorb within or just after the 50-μs pulse duration, even when τ is shorter than the pulse; for $\tau = 10^{-6}$ s, 17% of the dissolved molecules have not desorbed by the end of the gas pulse.[37]

In the opposite limit of large τ near 0.1 s, the desorption flux is spread over such a wide range of arrival times that the signal

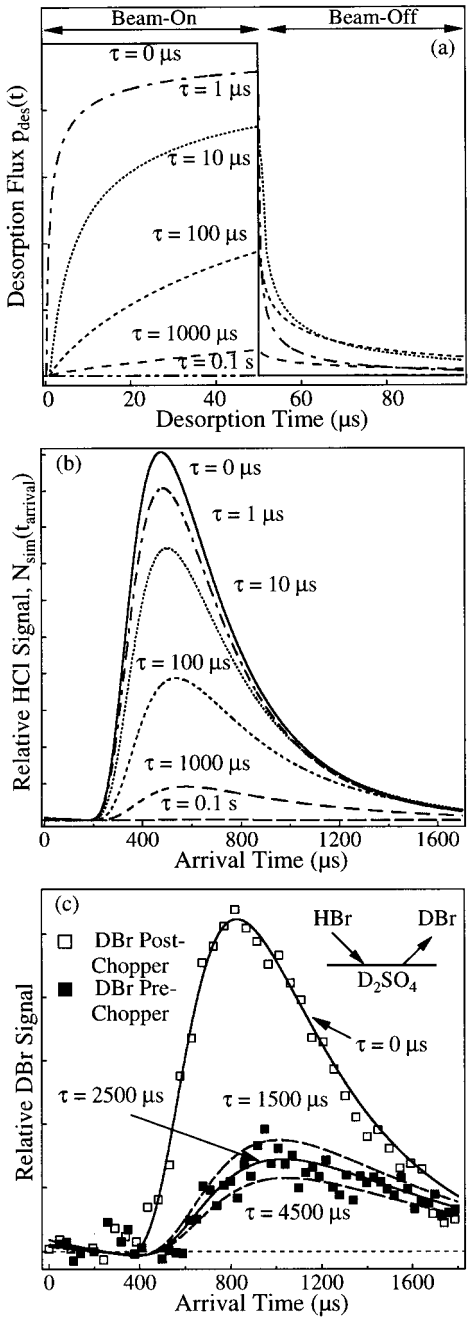

Figure 1. (a) Relative desorption flux $p_{des}(t)$ for gas molecules desorbing at time t during and after the 50-μs gas pulse. $p_{des}(t)$ depends only on the characteristic residence time τ. (b) Simulated pre-chopper TOF spectra for desorbing HCl obtained by convoluting $p_{des}(t)$ with a Maxwell−Boltzmann distribution at $T_{gly} = 273$ K. (c) Example of the fitting procedure for thermally desorbing DBr following collisions of HBr with 68.6 wt % D_2SO_4 at 213 K.

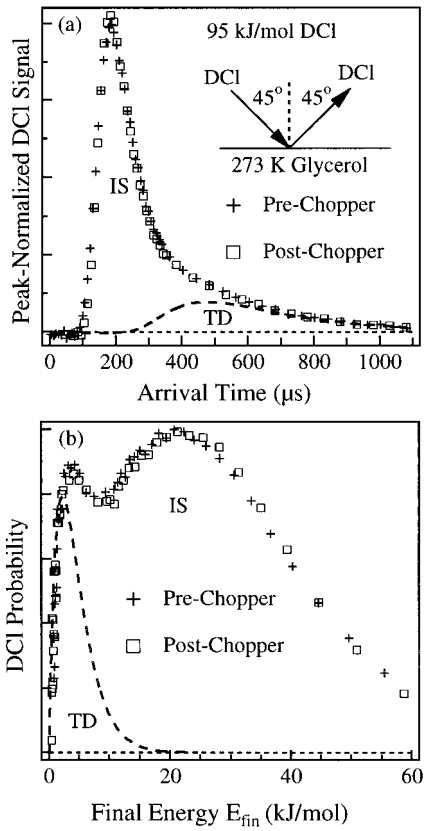

Figure 2. (a) Post- and pre-chopper TOF spectra for $D^{37}Cl$ following collisions of 95 kJ/mol DCl with glycerol at 273 K. There is no measurable intensity or arrival-time difference between the two spectra. IS and TD refer to inelastic scattering and thermal desorption. (b) Energy distributions obtained by direct inversion of the DCl TOF spectra in panel a.

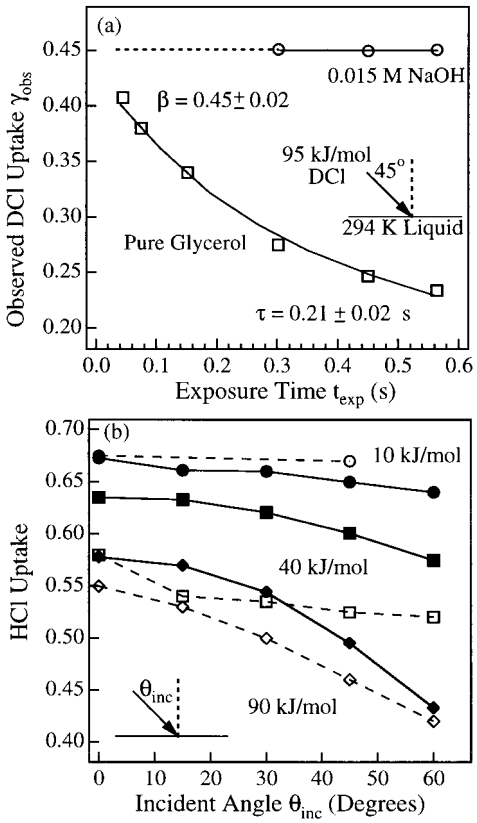

Figure 3. (a) Observed uptake of 95 kJ/mol DCl in pure glycerol (□) and in 0.015 M NaOH/glycerol (○) as a function of exposure time at 294 K. (b) Initial uptake β for HCl in pure glycerol (open symbols, reproduced from Figure 8 in the previous paper) and constant HCl uptake in 0.17 M NaOH/glycerol (solid symbols) at 294 K: 10 kJ/mol HCl (○, ●), 40 kJ/mol (□, ■), and 90 kJ/mol HCl (◇, ◆).

becomes uncorrelated with the incident gas pulses and merges with the background. In this case of longtime solvation, the pre-chopper desorption signal is too weak to extract the bulk solvation time. We instead determine τ by measuring gas uptake as a function of exposure time, as described in the preceding paper.

A demonstration of the pre-chopper fitting procedure is shown in panel c for HBr dissolving in 68.6 wt % D_2SO_4 at 213 K.[28] In this case, D^+ is in excess, and $p_{des}(t)$ depends only on the first power of $c(x = 0, t)/c^*$; the graphs of $p_{des}(t)$ and $N_{sim}(t_{arrival})$, however, remain similar to those in panels a and b.[28,33] A $\tau = 0$ curve is first scaled to the size of the DBr post-chopper spectrum, which is well fit by a Maxwell−Boltzmann distribution. We then adjust τ for a second curve until it matches the relative height and shape of the DBr pre-chopper spectrum. This procedure yields $\tau(\mathrm{DBr}) = 2.5\ (+2.0, -1.0) \times 10^{-3}$ s, which is close to the 2.0×10^{-3} s HBr residence time predicted by eq 2 of the preceding paper using literature values of $H^* = 4.1 \times 10^4$ M atm^{-1},[38] $D = 8.1 \times 10^{-9}$ cm^2 s^{-1},[39] and $\beta_{th} = 0.22$.[28]

We exploit two results from the residence time analysis in Figure 1b for DCl dissolving in glycerol: overlapping pre- and post-chopper spectra imply bulk residence times shorter than 10^{-6} s, and residence times longer than 10^{-1} s generate pre-chopper spectra of very low intensity.[33]

Residence Time for DCl Trapping and Desorption. We first determine the bulk residence time of impinging DCl molecules that do not undergo D → H exchange by comparing DCl post- and pre-chopper spectra. Panels a and b of Figure 2 plot TOF spectra and translational energy distributions of $D^{37}Cl$ exiting from 273 K glycerol after collisions of DCl at $E_{inc} =$ 95 kJ mol^{-1}. As described above, the IS component of the post-chopper spectrum is shifted to coincide with the pre-chopper IS component to cancel timing offsets and normalize intensities. Figure 2 shows that this shift also overlaps the spectra at the long arrival times and low final energies where thermal desorption occurs. The absence of a time or intensity shift in the thermal desorption region indicates that DCl molecules that undergo trapping and desorption without D → H exchange spend less than 10^{-6} s dissolved in glycerol. These DCl molecules appear to be propelled back into the gas phase by thermal motions of the surface molecules before they dissolve deeply enough to dissociate. If we assume that the diffusion coefficients for molecular DCl and Cl^- are both equal to 5×10^{-9} cm^2 s^{-1} at 273 K[40] and that the maximum solvation time is 10^{-6} s, then the average penetration depth of unexchanged DCl into bulk glycerol must be smaller than $(D_{HCl}\tau)^{1/2} \approx 10$ Å. These submicrosecond residence times have also been observed for HCl impinging on 70 wt % D_2SO_4 at 213 K at $E_{inc} = 100$, 42, and 14 kJ mol^{-1}, where overlapping post- and pre-chopper spectra of desorbing HCl were measured at each energy.[28]

DCl Uptake and Long-time Solvation. We next measured DCl uptake as a function of exposure time t_{exp} to determine the initial uptake $\beta(E_{inc}, \theta_{inc})$ and the characteristic time τ_{slow} for DCl molecules to dissociate, dissolve deeply into the bulk, and slowly desorb as HCl. This procedure is described in the preceding paper. The uptake data are shown in Figure 3a for DCl (□) at $E_{inc} = 95$ kJ mol^{-1}. The experiments were performed at 294 K instead of 273 K to lower the viscosity from 21 100 to 1300 cP and to enable the glycerol-covered wheel to be spun at rotation speeds up to 0.83 Hz and exposure times down to

0.045 s. The net uptake $\gamma_{obs}(t_{exp})$ is monitored at $^{35}Cl^+$ in the mass spectrometer and is therefore a measure of the total fraction of Cl^--containing species in solution and not of D → H exchange. The net uptake in Figure 3 decreases steadily with increasing t_{exp} because the dissolved Cl^- and D → H-exchanged H^+ are given more time to recombine and desorb. The solid-line fit to the data yields $\beta = 0.45 \pm 0.02$ and $\tau_{slow} = 0.21 \pm 0.05$ s, indicating that 45% of the impinging DCl molecules enter glycerol and remain within the liquid on average for 0.21 s before desorbing as HCl. On the basis of Figure 10 of the preceding paper, the incident DCl flux in the 95 kJ mol^{-1} beam is close to 1.0×10^{15} cm^{-2} s^{-1}.

Evidence for Rapid DCl → HCl Exchange. To determine if D → H exchange and desorption can occur on time scales much faster than the 0.2 s characteristic time measured above, we recorded the post- and pre-chopper spectra of HCl following collisions of DCl. Figure 1b predicts that HCl desorption should not be detectable in a pre-chopper spectrum for DCl molecules that dissociate and reside in glycerol with a characteristic residence time near 0.2 s (fewer than 0.1% of the HCl should desorb from the liquid during the 1800-μs recording time of the pre-chopper spectrum). Surprisingly, Figure 4a shows that the measured HCl pre-chopper desorption signal (○) is strong although significantly reduced from the post-chopper signal (□). The inelastic scattering signal at short times is due to a 6% HCl impurity in the incident DCl beam. It is removed by subtracting a pre-chopper spectrum (solid line) recorded under identical conditions using HCl as the incident gas beam. The impurity-subtracted spectra are shown in panel b. The predicted $\tau = 0.21$ s fit is indistinguishable from the baseline, whereas the measured HCl pre-chopper signal is 19% of the post-chopper signal. This HCl pre-chopper signal was not expected and was reproduced many times to confirm that it is real. The HCl desorption signal is also observable at 294 K, but it is more difficult to isolate because of the greater dissociative ionization of evaporating glycerol at the $H^{37}Cl$ mass.

We next attempted to fit the pre-chopper spectrum in Figure 4b with a single time distribution, assuming that solvation is controlled by a single residence time much shorter than the 0.2 s residence time measured in Figure 3a. The best fit to a single time distribution yields $\tau = 400$ μs. This fit matches the peak height but not the shape of the curve. Using eq 2 with $D_{HCl} = 5 \times 10^{-9}$ cm^2 s^{-1} at 273 K and a reactive flux F_{in} of 1×10^{15} cm^{-2} s^{-1}, we find that this 400-μs residence time corresponds to an equilibrium constant for HCl dissolution in glycerol of 40 M^2 atm^{-1}. This number is much smaller than the 2300 M^2 atm^{-1} value measured in the preceding paper at 294 K and the 19 000 M^2 atm^{-1} value predicted at 273 K.[41] It is also much smaller than the estimated equilibrium constant for HCl dissolution in ethylene glycol of 11 000 M^2 atm^{-1} at 273 K.[42] The single residence time fit of 400 μs therefore appears to be unreasonable, implying that the HCl pre-chopper signal in Figure 4b cannot be modeled by a single process with one characteristic residence time.

We instead model the HCl desorption signal in Figure 4 by assuming that two processes occur: solvation of Cl^- and D^+/H^+ for a characteristic residence time of 0.2 s and a rapid D → H exchange and HCl desorption process with a much shorter residence time. Because HCl molecules that undergo solvation for 0.2 s do not desorb on the time scale of the pre-chopper spectrum, we adjust the height of the simulated fit in Figure 4c to match the height of the measured pre-chopper spectrum. The best fit to the shape of the measured spectrum is given by $\tau = 0$ s, which is a Maxwell−Boltzmann distribution convoluted with the 50-μs beam pulse (fits with $\tau \leq 10^{-6}$ s are also reasonable). This analysis provides evidence that a fraction of the trapped DCl molecules (shown below to be ~7%) undergo submicrosecond solvation and D → H exchange. The time-dependent uptake data in Figure 3a and the post- and pre-chopper data in Figure 4c therefore imply that DCl solvation occurs on time scales of $<10^{-6}$ s and of 10^{-1} s.

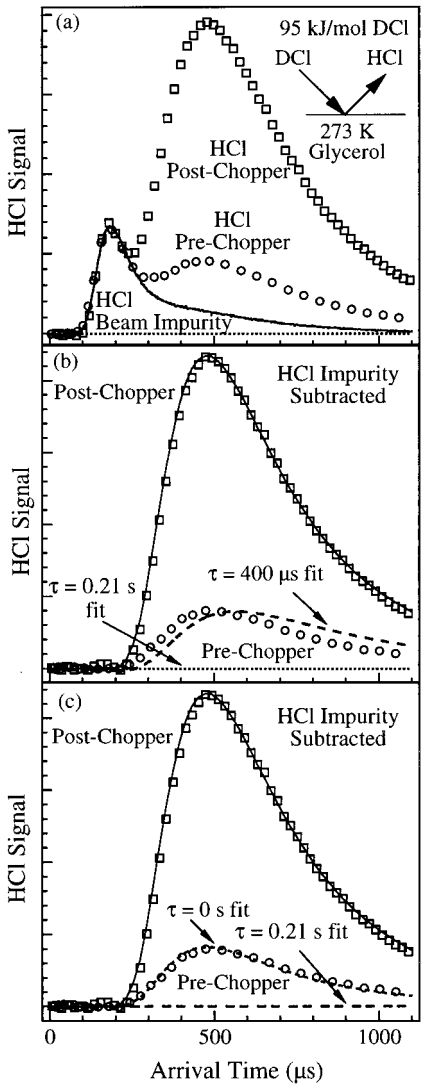

Figure 4. (a) Post- (□) and pre- (○) chopper TOF spectra of HCl after collisions of DCl with glycerol at 273 K. The solid line is the TOF spectrum of the 6% HCl contaminant in the incident beam, normalized to the IS peak of the post-chopper spectrum. (b) Post- and pre-chopper spectra after the HCl contaminant has been subtracted. The dashed line is a single component fit to the data using $\tau = 4 \times 10^{-4}$ s. The $\tau = 0.21$ s prediction is indistinguishable from the baseline. (c) The data are best fit by using a $\tau = 0$ s simulation and by assuming that HCl desorbs via one fast and one slow channel.

The assumption that HCl undergoes D → H exchange through distinct slow and fast channels is necessary to account for the time-dependent uptake measurements in Figure 3a (and in the preceding paper) that yield $\tau_{slow} = 0.2$ s and for the post-chopper and pre-chopper analyses in Figure 4c that yield $\tau_{fast} < 10^{-6}$ s. The determination that τ_{fast} is less than 10^{-6} s, however, is not robust because we matched only the shape and not the relative intensity of the pre-chopper spectrum. To measure τ_{fast} more precisely, we report the use of a chemical scavenging method below that isolates the fast signal and demonstrates that DCl molecules can indeed undergo exchange while dissolving in glycerol for less than 10^{-6} s.

DCl Uptake and Immediate Reaction in NaOH-Doped Glycerol Solutions. We investigated the time scale and mechanism for the rapid DCl → HCl exchange and desorption pathway by adding NaOH to glycerol and by monitoring the competition of H^+ and Cl^- recombination with H^+ and $C_3H_7O_3^-$ neutralization. Two solutions of 0.015 and 0.17 M NaOH in glycerol were prepared. The OH^- reacts with glycerol to produce $C_3H_7O_3^-$ and H_2O followed by water evaporation from solution before the scattering experiments are performed. The $C_3H_7O_3^-$ ions should react with D → H-exchanged H^+ and prohibit HCl desorption if the H^+ ions dissolve long enough to come into contact with $C_3H_7O_3^-$. The two pathways that compete for H^+ are

$$H^+(gly) + Cl^-(gly) \rightarrow HCl(g) \quad \text{recombination and desorption} \quad (3a)$$

$$H^+(gly) + C_3H_7O_3^-(gly) \rightarrow \text{glycerol} \quad \text{neutralization} \quad (3b)$$

The $C_3H_7O_3^-$ ions are on average ~4500 and ~400 Å apart, respectively, in the 0.015 and 0.17 M $C_3H_7O_3^-$ solutions. Rough estimates of the diffusion-limited time for neutralization can be obtained from $t_{neutral} \approx \{4\pi(D_{H^+} + D_{C_3H_7O_3^-})R_{ion}[C_3H_7O_3^-]\}^{-1}$.[43,44] Conductivity measurements show that H^+ and $C_3H_7O_3^-$ each diffuse anomalously rapidly in glycerol,[45] perhaps through a shuttling mechanism similar to the motions of H^+ and OH^- in water.[46] These measurements imply that D_{H^+} and $D_{C_3H_7O_3^-}$ are at least 10 times greater than $D_{Cl^-} \approx 5 \times 10^{-9}$ cm^2 s^{-1} at 273 K, yielding summed diffusion coefficients greater than 1×10^{-7} cm^2 s^{-1}.[47] We also use an effective ion−ion contact distance R_{ion} of 1×10^{-7} cm[48] and note that the near-interfacial concentration of $C_3H_7O_3^-$ is most likely depleted only in the outermost glycerol layer, as described in the Experimental Section. These numbers predict that the diffusion-limited neutralization times are ~10^{-6} and ~10^{-7} s for 0.015 and 0.17 M solutions, respectively. The diffusion depths $(D_{HCl}t_{neutral})^{1/2}$ corresponding to these times are smaller than 10 Å (two glycerol monolayers) into the bulk liquid. These shallow depths imply that all H^+ not confined to the near-interfacial region should be neutralized by $C_3H_7O_3^-$ ions. The use of NaOH as a filter to separate bulk and near-interfacial processes is confirmed below.

Irreversible Uptake in Basic Glycerol. Figure 3a illustrates the uptake of 95 kJ mol^{-1} DCl in the 0.015 M $C_3H_7O_3^-$ solution (○). The observed uptake of 0.45 is independent of exposure time, in sharp contrast to the time-dependent uptake of DCl in pure glycerol (□). This irreversible uptake is driven by the reaction of H^+ or D^+ with $C_3H_7O_3^-$ to produce neutral glycerol, leaving Na^+ and Cl^- in solution. Figure 3a shows that the initial uptake in pure glycerol and the constant uptake in 0.015 M $C_3H_7O_3^-$ are equal (each 0.45), indicating that virtually all H^+ ions dissolved in bulk glycerol are neutralized by $C_3H_7O_3^-$. However, repeated measurements using 0.17 M $C_3H_7O_3^-$ reveal that the uptake is slightly higher in this more basic solution. Figure 3b compares the initial uptake of 90, 40, and 10 kJ mol^{-1} HCl at $\theta_{inc} = 0-60°$ in pure glycerol with the constant HCl uptake in 0.17 M $C_3H_7O_3^-$ at 294 K. The irreversible uptake of HCl in 0.17 M $C_3H_7O_3^-$ is on average 0.04 ± 0.02 higher than the initial uptake in pure glycerol (90% confidence intervals for 12 measurements). A portion of these small differences is likely due to systematic errors in fitting the time-dependent uptake values, but the enhanced uptake in basic solution is corroborated by pre-chopper data shown later in Figure 6. This figure shows that the HCl desorption flux due to rapid exchange drops measurably when NaOH is added to pure glycerol.

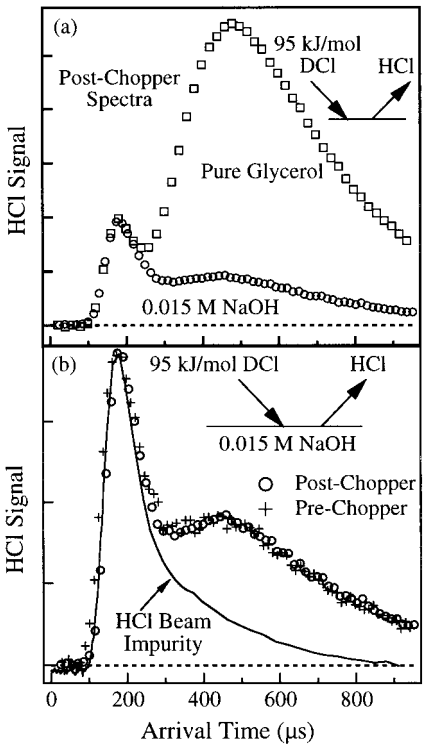

Figure 5. (a) Comparison of post-chopper TOF spectra of $H^{37}Cl$ desorbing from pure glycerol (□) and from 0.015 M NaOH/glycerol (○) at 273 K after collisions of 95 kJ/mol DCl. (b) Comparison of $H^{37}Cl$ post- and pre-chopper spectra after DCl collisions with 0.015 M NaOH/glycerol. The solid line is the pre-chopper spectrum of the 8% HCl impurity in the incident beam. The identical spectra indicate that the D → H-exchanged HCl molecules dissolve for less than 10^{-6} s in glycerol.

Together, these measurements imply that some D species (DCl, D^+) or H species (D → H exchanged-H^+, HCl) that would have taken part in the fast exchange process are instead captured by near-interfacial $C_3H_7O_3^-$ before they can leave the liquid. We use this observation below to help place an upper time limit on the rapid D → H exchange pathway.

HCl Desorption from NaOH-Doped Glycerol. The TOF spectra in Figure 5 confirm that bulk H^+ is neutralized by $C_3H_7O_3^-$, thereby suppressing HCl thermal desorption. Panel a shows post-chopper TOF spectra for HCl following collisions of DCl at 95 kJ mol^{-1} with pure glycerol and with 0.015 M $C_3H_7O_3^-$/glycerol at 273 K. The two post-chopper spectra have been normalized at the peaks of the inelastic scattering signals of the HCl impurity to scale the signals in two spectra recorded at different times and with potentially different incident DCl fluxes. Figure 5a shows that the HCl desorption signal drops significantly with addition of NaOH. This loss of HCl confirms that most DCl molecules that enter the liquid dissociate and react with $C_3H_7O_3^-$ before the Cl^- and D → H-exchanged H^+ combine and desorb as HCl. The HCl molecules that do desorb must therefore originate from DCl molecules that undergo immediate D → H exchange and desorption before they react with $C_3H_7O_3^-$ in solution. The similarity of the 5:1 signal ratios in Figures 4a and 5a is striking; in Figure 4a, the HCl desorption signal originating from bulk H^+ and Cl^- is suppressed by fast modulation of the DCl beam, and in Figure 5a, HCl desorption is suppressed by neutralization of bulk H^+ with $C_3H_7O_3^-$. The addition of NaOH therefore isolates the immediate exchange channel, allowing it to be observed in the absence of slow HCl desorption following bulk H^+ and Cl^- solvation.

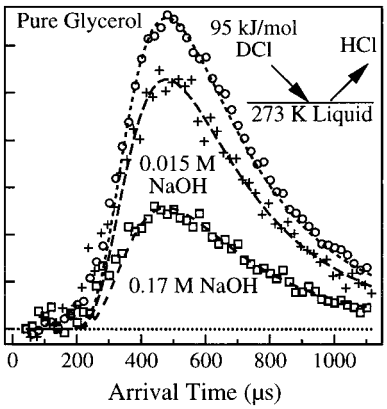

Figure 6. Comparison of pre-chopper spectra for HCl desorption following collisions of DCl with pure glycerol (○) and with 0.015 (+) and 0.17 M NaOH (□) in glycerol. The scattered HCl impurity signal has been subtracted from each spectrum (6% HCl impurity for experiments with pure glycerol and 8% HCl impurity for experiments with 0.015 and 0.17 M NaOH in glycerol). The lines are $\tau = 0$ s fits to each spectrum.

We next combine the fast modulation and NaOH doping techniques to determine an upper limit to the time for immediate DCl → HCl exchange. Figure 5b compares pre- and post-chopper spectra of D → H-exchanged HCl desorbing from the 0.015 M $C_3H_7O_3^-$ solution. This Figure shows that the HCl pre- and post-chopper spectra are identical to within the noise in the data. This important result demonstrates that the solvation time for D → H-exchanged HCl emerging from basic glycerol is less than 10^{-6} s on the basis of a comparison with the simulated TOF spectra in Figure 1b. *The overlap of the post- and pre-chopper spectra in Figure 5b is our most direct proof that significant D → H exchange and desorption can occur on a submicrosecond time scale*. For this rapid D → H exchange and HCl desorption channel, DCl/HCl diffusion into the bulk must be limited to depths smaller than $(D_{HCl}\tau_{fast})^{1/2} \approx 10$ Å.

Competition between Recombination and Neutralization. Figures 3 and 6 demonstrate that this immediate D → H exchange channel can itself be partially interrupted by $C_3H_7O_3^-$ ions in the near-interfacial region. As discussed above, Figure 3b shows that dissolved 0.17 M $C_3H_7O_3^-$ ions increase the overall uptake of DCl in glycerol by 0.04 ± 0.02 and specifically by 0.03 at $E_{inc} = 90$ kJ mol^{-1}. Figure 6 provides complementary evidence that this increase can be correlated with the removal of D^+/H^+ by $C_3H_7O_3^-$ ions. This Figure compares pre-chopper spectra of HCl desorbing from pure glycerol and from the 0.015 and 0.17 M $C_3H_7O_3^-$ solutions after collisions of 95 kJ mol^{-1} DCl. As in Figure 4b, the TOF spectra were scaled by the size of the HCl impurity in the 95 kJ mol^{-1} DCl incident beam, which was then removed from the spectra. The HCl desorption signal decreases by roughly 60% from pure glycerol to 0.17 M $C_3H_7O_3^-$. As we show below, the absolute probability for the immediate exchange channel is 0.043 for 95 kJ mol^{-1} DCl at $\theta_{inc} = 45°$. The 60% reduction in the HCl desorption signal should correspond to an increase in DCl uptake of $0.60 \times 0.043 = 0.026$, which is close to the 0.03 change in HCl uptake at 90 kJ mol^{-1} measured in Figure 3b. These similar numbers provide further evidence that a significant fraction of the DCl molecules undergoing immediate exchange can be captured by near-interfacial $C_3H_7O_3^-$ before they can escape as HCl. This 60% capture rate suggests that H^+ and Cl^- recombination occurs on a time scale similar to that of H^+ and $C_3H_7O_3^-$ neutralization. This neutralization time was estimated above to be approximately 10^{-7} s, supporting the submicrosecond reaction times implied by Figures 4c and 5b.

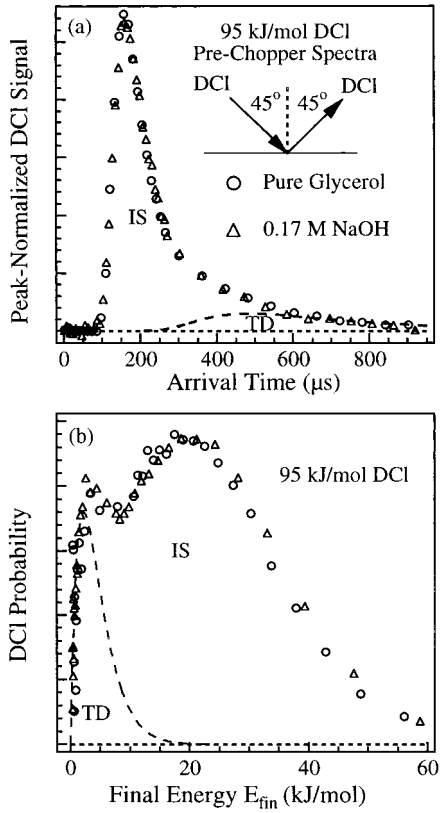

Figure 7. Comparison of (a) pre-chopper spectra and (b) energy distributions for $D^{37}Cl$ following collisions of 95 kJ/mol DCl with pure glycerol and 0.17 M NaOH in glycerol. The overlapping spectra indicate that thermalized DCl molecules that do not exchange do not react with $C_3H_7O_3^-$ ions.

No Evidence for D^+ and Cl^- Recombination. The NaOH-doped glycerol may also be used to investigate whether some DCl molecules dissociate in the near-interfacial region, followed by D^+ and Cl^- recombination and DCl desorption before the D^+ ions undergo exchange. Figure 7 displays TOF spectra of DCl scattering from pure glycerol and the 0.17 M $C_3H_7O_3^-$ solution at $E_{inc} = 95$ kJ mol^{-1}. Although the thermal desorption intensity is small at this high collision energy, there appears to be no change in DCl desorption flux from the pure and basic liquids in contrast to that of the DCl → HCl channel in Figure 6. The identical TOF spectra in Figure 7 indicate that any recombination of D^+ and Cl^- and desorption of DCl before D → H exchange must either be very small or much faster than the immediate D → H exchange channel. One such fast process is geminate recombination of D^+ and Cl^-, whose subpicosecond time scale cannot be measured in these experiments.[49] In the absence of this ultrafast recombination, the DCl thermal-desorption channel should be dominated by physical trapping and rapid desorption of DCl molecules before they are able to dissociate.

Scattering, Desorption, Solvation, and Reaction Probabilities. We can combine the DCl uptake and TOF measurements to determine the absolute probabilities for direct inelastic scattering ($p_{scatter}$), overall trapping (p_{trap}), trapping−desorption ($p_{trap-desorb}$), immediate exchange and desorption (p_{ied}), and solvation (p_{solv}) for DCl striking glycerol. The DCl trapping probability is the sum of the solvation, trapping−desorption, and immediate exchange−desorption probabilities:

$$p_{trap}(E_{inc}, \theta_{inc}) = p_{solv} + p_{trap-desorb} + p_{ied} \qquad (4a)$$

and

$$p_{scatter}(E_{inc}, \theta_{inc}) = 1 - p_{trap}(E_{inc}, \theta_{inc}) \quad (4b)$$

Detailed calculations of each probability are described in Appendix I. Briefly, the DCl uptake measurements in Figure 3a yield $p_{solv} = \beta(E_{inc}, \theta_{inc})$ and the bulk residence time τ_{slow} for the slow desorption channel. This solvation probability includes those DCl molecules that enter the bulk as molecular DCl or as ions after dissociating in the interfacial region. We then assume that the DCl and HCl molecules desorb with the same angular distributions and compare the DCl and HCl desorption signals in Figures 2a and 4c to determine the relative probabilities for trapping−desorption and immediate exchange−desorption, respectively. The relative probabilities are converted to absolute probabilities by anchoring them to the gas uptake measurements in Figure 3a. Equation 4a then yields the total trapping probability, and eq 4b determines the total inelastic scattering probability, integrated over all exit angles.

The different pathways for DCl collisions with glycerol at E_{inc} = 95, 53, and 14 kJ mol^{-1} are shown in the scattering diagrams in Figure 8. The incident angle θ_{inc} is 45° and the exposure time t_{exp} is 0.45 s in each case. The fractions in parentheses are the probabilities for each process. The percentages listed above these fractions are $100(p_{process}/p_{trap})$. These percentages reveal the competition among the bulk solvation, immediate desorption, and immediate exchange processes for thermally equilibrated DCl molecules. The scattering diagrams show that, even at high collision energies of 95 and 53 kJ mol^{-1}, most DCl molecules thermally equilibrate at the surface of glycerol ($p_{trap} > 0.5$), and most of these enter the liquid and dissolve for long times ($p_{solv}/p_{trap} > 70\%$). As discussed in the preceding paper, p_{trap} increases as E_{inc} decreases and is close to 0.9 at 14 kJ mol^{-1}. The trapping probability is likely to be even closer to 1 at thermal impact energies of $2RT_{gly}$ = 4.5 kJ mol^{-1} at 273 K. At all three collision energies, fewer molecules scatter from the surface than dissolve in the bulk ($p_{scatter} < p_{solv}$). Trapping−desorption is also less likely than solvation ($p_{trap-desorb} < p_{solv}$). The immediate exchange and desorption process occurs least often but is significant enough to measure for the high beam fluxes produced by the 53 and 95 kJ mol^{-1} beams. We were not able to characterize this channel quantitatively at E_{inc} = 14 kJ mol^{-1} because of the low flux of this N_2-seeded beam. As described in Appendix I, we set p_{ied}/p_{trap} equal to the value of 7% at 95 kJ mol^{-1} and solved for the other probabilities at E_{inc} = 14 kJ mol^{-1} using this value.

Events that occur after trapping should be independent of DCl impact energy and approach angle because molecules that thermally equilibrate at the surface lose the memory of their initial trajectory. One way to test if trapping precedes reaction and immediate desorption is to determine if the branching fractions for trapping−desorption, immediate exchange and desorption, and longtime solvation are independent of E_{inc}. These fractions are equal to $p_{process}/p_{trap}$ and are listed in Figure 8 as percentages. The similar percentages at 95, 53, and 14 kJ mol^{-1} confirm that DCl molecules thermalize upon collision before they desorb or undergo interfacial or bulk reaction. For those DCl molecules that thermally equilibrate at the surface, 19−21% desorb as DCl, and 7−8% undergo D → H exchange and then desorb, each after dissolving for less than 10^{-6} s. The remaining 73−76% of the thermalized DCl molecules enter glycerol for long times, accompanied by dissociation and D → H exchange. For the DCl−glycerol system, therefore, roughly

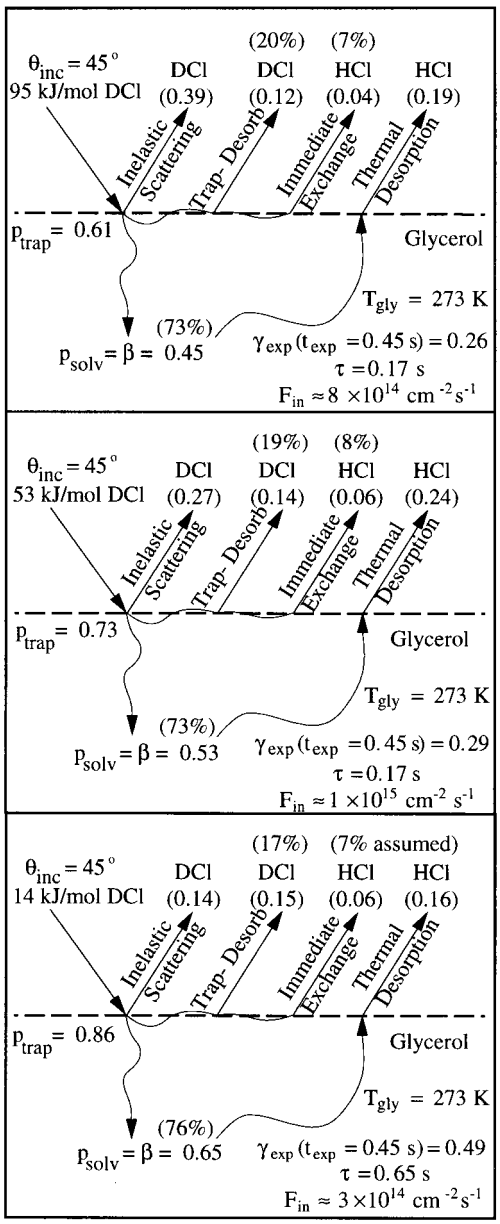

Figure 8. Scattering pathways for DCl collisions with liquid glycerol at θ_{inc} = 45° and at E_{inc} = 95, 53, and 14 kJ/mol. The probabilities for each pathway are listed in parentheses. The percentages are equal to $100(p_{process}/p_{trap})$.

1 in 10 DCl molecules that undergo D → H exchange does so by reacting solely in the near-interfacial region of the protic liquid.

Discussion: Interfacial and Bulk Solvation of DCl in Glycerol

DCl Trapping and Dissociation. In the first step toward reaction, the impinging DCl molecules must dissipate their excess kinetic energy and thermally equilibrate in the surface region. This trapping requirement is based on the observation above that the solvation, immediate exchange, and immediate desorption probabilities do not depend on the incident energy E_{inc}. We also showed in the preceding paper that the trapping probabilities decrease steadily as E_{inc} increases, indicating that DCl molecules thermalize more readily when they have less energy to dissipate. At thermal collision energies of $2RT_{gly}$ = 4.5 kJ mol^{-1} at 273 K, 90% or more of the incident DCl molecules are expected to thermalize (because $p_{trap}(E_{inc}$ = 14

kJ mol^{-1}) > 0.85), and 80% of these go on to react ([p_{ied} + p_{solv}]/p_{trap} ≈ 0.8).

Figures 2 and 7 show that the 20% of the thermalized DCl molecules that do not react enter glycerol for less than 10^{-6} s and are unaffected by the presence of $C_3H_7O_3^-$. Unless these molecules dissociate and geminately recombine, it is likely that they are propelled back into the gas phase immediately after they thermally equilibrate on the surface. These impinging DCl molecules may avoid reaction because they happen to interact primarily with CH_2 and CH groups that occupy 40% of the surface of glycerol[50] or because they desorb before reorienting into favorable hydrogen-bonding configurations with surface OH groups.

The remaining 80% of the thermally accommodated DCl molecules undergo D → H exchange. We imagine that these molecules bind initially to surface OH groups of glycerol through one strong $ClD\cdots OC_3H_7O_2$ and one weak $DCl\cdots HOC_3H_7O_2$ hydrogen bond.[10,12,16,51,52] The surface residence time may be roughly estimated by assuming that the binding energy of HCl to ice, of approximately 23 to 33 kJ mol^{-1},[16,53] also applies to HCl adsorption on glycerol. These adsorption energies predict surface residence times of $\tau_{surf} \approx \tau_0 e^{-E_{ads}/RT}$ that are less than 2×10^{-7} s at 273 K, assuming that τ_0 is 10^{-13} s.

During this submicrosecond adsorption time, DCl molecules that do not desorb may tumble along the surface and perhaps submerge just under the outermost glycerol layer, reorienting into configurations that pull the DCl deeper into the liquid or that initiate interfacial D^+ Cl^- ion-pair formation. These ions may then begin to separate and move deeper into the bulk region, accompanied by $D^+ \rightarrow H^+$ exchange with the OH groups of adjacent glycerol molecules. This deep diffusion accounts for 73% of the initially adsorbed DCl molecules. The preceding paper shows that a Cl^- ion diffusing into the bulk does not recombine with its D → H-exchanged H^+ partner but instead combines eventually with an H^+ originating from another DCl molecule. The originally paired H^+ and Cl^- must therefore separate widely as they diffuse for times from 10^{-1} to 10^0 s, reaching depths $(D_{HCl}\tau_{slow})^{1/2}$ of more than 2000 Å for $D_{HCl} = 5 \times 10^{-9}$ cm^{-2} s^{-1} at 273 K.

The bulk residence time measurements of 10^{-1} to 10^0 s yield only the longest solvation time in a multistep process. In particular, these measurements do not reveal if the Cl^- and D^+/H^+ ions that undergo longtime solvation are first formed in the interfacial region or if DCl diffuses several monolayers before dissociating. The existence of a submicrosecond D → H exchange channel, however, limits the bulk diffusion depth to which dissociation and recombination must occur to within $(D_{HCl}\tau_{fast})^{1/2}$ < 10 Å for the 7−8% of the thermalized DCl molecules that follow this channel. When added to the interfacial thickness of 5 Å,[50] the estimated reaction region for these molecules is approximately 15 Å from the surface, corresponding to three glycerol molecules. As mentioned in the Introduction, this potentially facile, surface-to-near-interfacial dissociation of DCl is supported by quantum calculations of HCl embedded in water clusters, which predict that HCl dissociates when surrounded by only four water molecules,[1−7] and by the dissociation of HCl on or within the first bilayer of ice.[10−12]

Mechanism for Rapid D → H Exchange. The most startling aspect of HCl dissolution in glycerol is the observation that 7−8% of the thermalized DCl molecules undergo D → H exchange and desorption while spending less than 10^{-6} s dissolved in the bulk liquid. The nearly complete overlap of the post- and pre-chopper HCl desorption signals in Figure 5 suggests that there is no measurable bulk diffusion and therefore

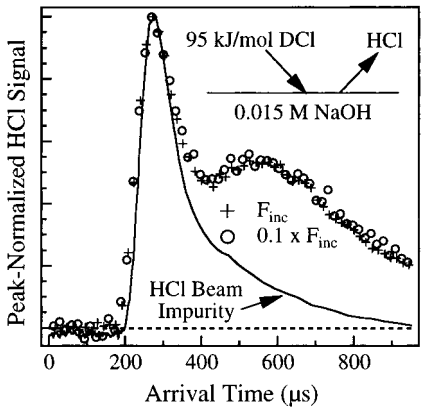

Figure 9. Pre-chopper spectra of HCl following collisions of 95 kJ/mol DCl with 0.015 M NaOH in glycerol. The fluxes differ by 10 in the two DCl incident beams. The solid line is the pre-chopper spectrum of the 8% HCl impurity in the incident DCl beam. The identical spectra indicate that the immediate HCl desorption signal scales linearly with the incident DCl flux.

that exchange occurs at or just below the surface of glycerol. This process occurs even in the midst of massive DCl solvation in bulk glycerol (p_{solv} = 0.73), which is exothermic by approximately 67 kJ mol^{-1} and is very favorable (K_{HCl}(gly) ≈ 15 000 M^2 atm^{-1} at 273 K). We note that interfacial D → H exchange has also been observed from differences in the uptake of normal (5.7% at 291 K) and deuterated ethanol (10.5%) in water, where the higher uptake of CH_3CH_2OD indicates that interfacial D → H exchange and desorption is as likely as bulk solvation.[24]

We envision three different mechanisms for immediate DCl → HCl exchange and desorption: (1) DCl dissociation in the near-interfacial region, followed by $D^+ \rightarrow H^+$ exchange and rapid, diffusion-controlled recombination of H^+ and Cl^- originating from different DCl molecules; (2) DCl dissociation, $D^+ \rightarrow H^+$ exchange, and H^+ and Cl^- recombination originating from the same DCl molecule within a cage of glycerol molecules near the interface; and (3) neutral and concerted DCl → HCl exchange near the interface.

Evidence against near-interfacial, diffusion-controlled recombination of H^+ and Cl^- was obtained by measuring the dependence of the pre-chopper HCl desorption signal on the incident DCl flux F_{inc}. We focus on the flux dependence because we learned in the preceding paper that the rate of HCl desorption after longtime Cl^- and H^+ solvation depends on the product of the equal Cl^- and H^+ concentrations. This quadratic dependence implies that the Cl^- and H^+ ions that recombine and desorb as HCl must originate from separate HCl molecules and are not ions that are originally part of the same HCl molecule. For the short reaction times in the immediate exchange pathway, the product $[H^+][Cl^-]$ scales approximately as F_{inc}^2.[54] If we observe an HCl flux dependence close to F_{inc}^2, then the DCl molecules responsible for rapid HCl desorption must first dissociate near the surface, followed by immediate recombination of Cl^- and D → H-exchanged H^+ originating from separate DCl molecules.

Figure 9 shows the effect of DCl flux on the pre-chopper HCl desorption signal from 0.015 M $C_3H_7O_3^-$ in glycerol. The combined use of pre-chopper modulation and the basic solution ensures that the HCl desorption signal arises solely from the immediate exchange channel. The DCl flux was varied by a factor of 10, from approximately 10^{15} to 10^{14} cm^{-2} s^{-1}, by increasing the distance between the molecular beam nozzle and the glycerol surface. The pre-chopper TOF spectra are normalized at the inelastic scattering peaks of the constant 8% HCl

impurity. This normalization scales the TOF spectra to the incident flux and allows the HCl desorption signals to be directly compared. There is no measurable difference in the TD intensity, indicating that the HCl desorption flux due to rapid exchange is a constant fraction of the incident DCl flux and therefore increases with F_{inc} and not with F_{inc}^2.

The observation that the immediate HCl desorption flux scales linearly with F_{inc} rules out a mechanism in which the DCl molecules dissociate in the interfacial region and a portion proportional to F_{inc}^2 recombine diffusively and desorb before they are neutralized by $C_3H_7O_3^-$. We describe below a caging mechanism for rapid D → H exchange that is consistent with the observation that the HCl pre-chopper desorption flux depends linearly on F_{inc}. A second, less-likely mechanism is presented in Appendix II, which shows that very fast diffusion of H^+ and Cl^- would also lead to a linear relation between F_{inc} and the HCl desorption flux.

Interfacial Caging Model. This mechanism is constructed by interpreting the linear flux dependence in Figure 9 to imply that H^+ and Cl^- ions that recombine immediately into HCl originate from the same DCl molecule and not from two separated DCl molecules. A single DCl molecule is first captured within a partial or complete cage of glycerol molecules at or just below the outermost layer of glycerol molecules. The initial formation of a $Cl^-\cdot{}^+DHOC_3H_7O_2$ ion pair should be aided by neighboring OH groups that partially or completely solvate the ions. Ball and stick models suggest that full solvation of the ion pair (three additional hydrogen bonds to Cl^- and one additional hydrogen bond to $^+$DHOC—) requires that OH groups from at least two more glycerol molecules orient toward the $Cl^-\cdot{}^+DHOC_3H_7O_2$ structure. Ionization would then be followed by D → H exchange:

$$\mathbf{D}Cl + (C_3H_8O_3)_n \rightarrow [Cl^-\cdot{}^+\mathbf{D}HOC_3H_7O_2](C_3H_8O_3)_{n-1} \quad \text{ion pair formation} \quad (5a)$$

followed by

$$\rightarrow [Cl^-\cdot{}^+H\mathbf{D}OC_3H_7O_2](C_3H_8O_3)_{n-1} \rightarrow HCl + C_3H_7\mathbf{D}O_3(C_3H_8O_3)_{n-1} \quad \text{D} \rightarrow \text{H interchange} \quad (5b)$$

or

$$\rightarrow [Cl^-\cdot{}^+H_2OC_3H_7O_2]C_3H_7\mathbf{D}O_3(C_3H_8O_3)_{n-2} \rightarrow HCl + C_3H_7\mathbf{D}O_3(C_3H_8O_3)_{n-1} \quad H^+ \text{ shuttling} \quad (5c)$$

Interchange between H and D atoms (pathway 5b) within the ion pair transforms the $Cl^-\cdot D^+$ complex into $Cl^-\cdot H^+$ during its lifetime in the cage, followed by formation of molecular HCl. These motions may be more extended, and the initial $Cl^-\cdot{}^+DHOC_3H_7O_2$ complex may first transfer H^+ to a neighboring —COH group, allowing H^+ to shuttle among OH groups within the solvent cage before it recombines with Cl^- to generate desorbing HCl (pathway 5c). The reduction in the immediate HCl desorption flux observed in Figure 6 by adding NaOH suggests that the ions must remain clustered near the surface long enough for $C_3H_7O_3^-$ to capture approximately half of the D^+ or H^+ in 0.17 M $C_3H_7O_3^-$ solutions, a process estimated above to occur in 10^{-7} s. We also note that the reverse of 5a allows reformation and escape of DCl, a process that we cannot distinguish from DCl trapping and immediate desorption.

The remaining 73% of the DCl molecules that dissolve for long times may pass through the interface intact and dissociate several monolayers deep, or as discussed above, they may also dissociate near the surface. These Cl^- and D^+ or D → H-exchanged H^+ ion pairs would then break out of the initial glycerol cage and diffuse separately and for long times into the bulk. This escape may evolve naturally as glycerol molecules intervene between the Cl^- and $^+DHOC_3H_7O_2$ ions, eventually leading to further separation and longtime diffusion of the ions through the liquid. By analogy with the predicted mechanism for HCl dissociation in water,[8] the branching between immediate Cl^- and H^+ recombination and ion separation may be controlled by the ability of the solvent glycerol molecules to reorient into positions that separately solvate the Cl^- and D^+/H^+ ions. After this longtime solvation, the ions would eventually diffuse to the near-interfacial region where Cl^- and H^+ originating from separate DCl molecules then recombine within a cage of glycerol molecules and desorb before dissociation occurs again.

It is also possible that immediate D → H exchange proceeds not by DCl dissociation and H^+ and Cl^- recombination within the glycerol cage but by a neutral and concerted bond switching between a DCl molecule and one or more surrounding HO groups. Although these reactions often have high barriers,[55] concerted D → H exchange might be favored at the outermost region of the interface where Cl^- and D^+ are not as well solvated as in interior regions. This neutral path also provides a way by which DCl can be converted to HCl without competition from Cl^- and D^+/H^+ diffusion out of the initial cage. Experiments are underway to investigate the ionic nature of the rapid exchange process by measuring the effects of added salt on the rate of immediate exchange. In either the ionic or neutral pathway, however, the observation that ~7% of the DCl molecules exchange immediately and ~73% dissolve for long times implies that 1 in 10 reacting molecules undergoes exchange near the surface and without dipping deeply into the bulk region for extra solvation.

Summary and Conclusions

The existence of rapid, near-interfacial DCl → HCl exchange and desorption in the midst of massive and longtime bulk solvation of H^+ and Cl^- is the most startling outcome of these investigations. Figure 8 summarizes the main results: among the impinging DCl molecules that thermally equilibrate at the surface of glycerol, ~7% undergo D → H exchange and HCl desorption while dissolving for less than 10^{-6} s, 20% desorb without exchange on the same or on a shorter time scale, and the remaining 73% dissolve deeply into the bulk as Cl^- and D → H-exchanged H^+ for long times. The linear flux dependence of the immediate exchange and desorption channel is consistent with a mechanism in which rapid D → H exchange occurs between a DCl molecule and HO groups within a near-interfacial cage of glycerol molecules. This exchange may occur through DCl ionization, $D^+ \rightarrow H^+$ exchange, and $H^+ + Cl^-$ recombination and immediate desorption or through a neutral bond switching between DCl and glycerol OH groups.

Our investigations of DCl and HCl in glycerol, in conjunction with previous studies of HCl in water, highlight the diverse range of initial interactions of acidic gases with neutral, hydrogen-bonding liquids. The probability that thermally impinging HCl molecules enter the bulk region of water at 293 K is measured to be only 0.06−0.1,[22,23] which is at least seven times lower than for HCl striking glycerol (this entry encompasses HCl molecules that enter the solvent intact or as $Cl^- + H^+$ after dissociation at the interface). It is not known whether the immediate exchange and desorption pathway exists for the HCl−water system (as it does for ethanol−water[24]), but the comparison of entry probabilities implies that surface glycerol

molecules are much more efficient than surface water molecules in providing a gateway into the bulk liquid for HCl. We do not know if these differences arise from the higher vapor pressure of water and its wider and more mobile interfacial region or if the OH groups of glycerol provide better initial binding sites than do the OH groups of water.[56] Despite the lower exothermicity and solubility of HCl in glycerol than in water, glycerol appears to dissolve HCl 10 times more readily, suggesting that trends in bulk solvation cannot always be used to predict trends in interfacial reactivity.

Appendix I: Calculation of Scattering, Trapping, and Reaction Probabilities

The individual probabilities in eqs 4a and b for solvation (p_{solv}), immediate exchange (p_{ied}), and trapping and immediate desorption ($p_{trap-desorb}$) are calculated from the following equations, which are explained below. In experiments reported here, t_{exp} is equal to 0.45 s, and θ_{inc} is equal to 45°.

$$p_{solv}(E_{inc}, \theta_{inc}) = \beta(E_{inc}, \theta_{inc}) \tag{A.1}$$

$$p_{ied} = \left[\frac{I_{pre}^{HCl}}{I_{post}^{HCl}(t_{exp}) - I_{pre}^{HCl}}\right](\beta(E_{inc}, \theta) - \langle\gamma_{exp}(t_{exp})\rangle) \tag{A.2}$$

$$p_{trap-desorb} = \left[\frac{I_{post}^{DCl}(t_{exp})}{I_{post}^{HCl}(t_{exp}) - I_{pre}^{HCl}}\right](\beta(E_{inc}, \theta) - \langle\gamma_{exp}(t_{exp})\rangle) \tag{A.3}$$

where

$$\langle\gamma_{exp}(t_{exp})\rangle = (1/t_{exp})\int_0^{t_{exp}}\gamma_{exp}(t)\,dt \tag{A.4}$$

and

$$\gamma_{exp}(t) = \beta(E_{inc}, \theta_{inc})[1 - c(x = 0, t)^2/c^{*2}] \tag{A.5}$$

The probability $p_{solv}(E_{inc}, \theta_{inc})$ that a DCl molecule enters bulk glycerol as either molecular DCl or as Cl^- and D^+ or H^+ is equal to the initial uptake, $\beta(E_{inc}, \theta_{inc})$. This initial value is extracted from measurements of the observed uptake as a function of exposure time, $\gamma_{obs}(t_{exp})$ versus t_{exp}, like that shown in Figure 3. These measurements also yield the characteristic residence time τ_{slow} for the slow desorption channel.

The probability p_{ied} for immediate DCl → HCl exchange and HCl desorption is proportional to the HCl pre-chopper desorption signal in Figure 4b. We calculate p_{ied} in the following way. The pre- and post-chopper desorption fluxes I_{pre}^{HCl} and $I_{post}^{HCl}(t_{exp})$ are obtained by integrating the mass spectrometer signals $N(t)$ according to $I = \int_0^\infty[N(t)/t]\,dt$. These fluxes are then related to the DCl uptake measurements, which anchor them to an absolute probability. The quantity $\langle\gamma_{exp}(t_{exp})\rangle$ is the probability that DCl molecules dissolving in glycerol between $t = 0$ and $t_{exp} = 0.45$ s are still in the bulk liquid at t_{exp} as Cl^- and D → H-exchanged H^+. This quantity is determined using eqs A.4 and A.5 and the measured values of β and τ_{slow}. The difference $[\beta(E_{inc}, \theta_{inc}) - \langle\gamma_{exp}(t_{exp})\rangle]$ is therefore the probability that H^+ and Cl^- have reformed into HCl and have desorbed by time t_{exp}. The HCl post-chopper desorption signal in Figure 4c (with flux $I_{post}^{HCl}(t_{exp})$) is the sum of the desorption signals due to the slow recombination of dissolved H^+ and Cl^- and to the fast exchange and desorption process (with flux I_{pre}^{HCl}). However, $[\beta(E_{inc}, \theta_{inc}) - \langle\gamma_{exp}(t_{exp})\rangle]$ is proportional only to the slow desorption channel, the difference $[I_{post}^{HCl}(t_{exp}) - I_{pre}^{HCl}]$, because the fast exchange and desorption channel is a separate, additional process and not part of the slow process characterized by τ_{slow}. Therefore, the ratio of probabilities $p_{ied}/[\beta(E_{inc}, \theta_{inc}) - \langle\gamma_{exp}(t_{exp})\rangle]$ is equal to the ratio of desorption fluxes $I_{pre}^{HCl}/[I_{post}^{HCl}(t_{exp}) - I_{pre}^{HCl}]$, yielding eq A.2. Parallel arguments lead to the expression for $p_{trap-desorb}$.

Uptake and intensity data for 95 kJ mol^{-1} DCl at $t_{exp} = 0.45$ s and $\theta_{inc} = 45°$ are used to illustrate the calculations. We use $\beta = 0.45 \pm 0.02$ measured at 294 K rather than at 273 K because of difficulties in making uptake measurements at the high speeds (low t_{exp}) of the liquid-coated disk through highly viscous glycerol at 273 K. However, Figure 5 of the preceding paper indicates that β varies by less than 0.02 from 294 to 273 K. The value of τ_{slow} at 273 K was then determined by measuring the uptake, $\gamma_{obs}(t_{exp} = 0.45\text{ s})$, of 0.19 ± 0.02 at a single slow wheel speed of 0.083 Hz and fitting β and γ_{obs} to a characteristic residence time of 0.21 ± 0.05 s. These values yield an average uptake within the exposure region, $\langle\gamma_{exp}(t_{exp} = 0.45\text{ s})\rangle$, of 0.26 ± 0.01 using eqs A.4 and A.5. The ratios of TOF intensities in brackets in eqs A.2 and A.3 are determined from Figures 2a and 4b to be 0.226 and 0.622, respectively. These numbers yield a bulk solvation probability for DCl of $p_{solv} = 0.45 \pm 0.02$, an immediate exchange and desorption probability p_{ied} of 0.043 ± 0.005, a trapping−desorption probability $p_{trap-desorb}$ of 0.12 ± 0.01, a total trapping probability p_{trap} of 0.61 ± 0.03, and a direct scattering probability p_{scat} of 0.39 ± 0.03. The error bars were calculated by propagating the uncertainties in β and γ_{obs} of ± 0.02 each. The probabilities are displayed in the scattering diagram in Figure 8a, and the analogous probabilities for $E_{inc} = 53$ kJ mol^{-1} are shown in Figure 8b.

We were unable to measure I_{pre}^{HCl} precisely for $E_{inc} = 14$ kJ mol^{-1} because of the low flux of this near-thermal beam. However, we did measure the ratio $I_{post}^{DCl}(t_{exp})/I_{post}^{HCl}(t_{exp})$ of 0.68 and $\gamma_{obs}(t_{exp})$ of 0.43 ± 0.03 at $t_{exp} = 0.45$ s. These values permit an estimate of $p_{trap-desorb}$ if we assume that $p_{ied}/p_{trap} \approx 0.07$ and that $\beta(14\text{ kJ mol}^{-1}, 45°) \approx 0.65$ on the basis of the measured value for HCl at $E_{inc} = 10$ kJ mol^{-1} in Figure 3. These measurements yield $\tau = 0.65$ s and $\langle\gamma_{exp}(t_{exp} = 0.45\text{ s})\rangle = 0.49$. Equation A.3 may be rewritten as

$$p_{trap-desorb} = \left[\frac{I_{post}^{DCl}(t_{exp})}{I_{post}^{HCl}(t_{exp})}\right](\beta(E_{inc}, \theta) - \langle\gamma_{exp}(t_{exp})\rangle + p_{ied})$$

and combined with eq 4a to yield $p_{trap} \approx 0.87$, $p_{solv}/p_{trap} \approx 0.75$, and $p_{trap-desorb}/p_{trap} \approx 0.18$. These results indicate that nearly all DCl molecules thermally equilibrate after collisions at 14 kJ mol^{-1} and that the fractions of DCl molecules that desorb as DCl or that dissolve for long times are similar to the fractions at higher collision energies.

Appendix II: Interfacial H^+ and Cl− Diffusion Mechanism for Fast D → H Exchange

The linear flux dependence in Figure 9 is also consistent with a mechanism in which a *fixed*, ~7% fraction of the adsorbed DCl molecules dissociate, diffuse rapidly as ions near the interface, and recombine as HCl. If the fraction of molecules that dissociate near the interface is independent of F_{inc}(DCl) and if all ions recombine within the experimental measurement time t_{meas}, then the immediate HCl desorption flux would be a fixed fraction of the incident DCl flux, as observed in Figure 9. All Cl^- and H^+ ions must diffuse, recombine, and desorb within t_{meas} in this model; if some near-interfacial ions remain for longer than t_{meas}, then F_{des}(HCl) would decrease nonlinearly with a drop in F_{inc}(DCl) because of longer HCl residence times at lower DCl flux.

We do not know our experimental time resolution for reactions occurring at or just below the surface (the τ values in Figure 1 refer to bulk solvation), but it must be smaller than the DCl pulse duration of 5×10^{-5} s. However, even this conservative estimate of t_{meas} requires very high interfacial mobilities of H^+ and Cl^-. For the lower incident flux of 1×10^{14} cm^{-2} s^{-1}, $t_{meas} = 5 \times 10^{-5}$ s, and $D_{HCl} = 5 \times 10^{-9}$ cm^{-2} s^{-1}, the interfacial ion concentration is $(0.07F_{inc}t_{meas})/(D_{HCl}t_{meas})^{1/2} = 7 \times 10^{14}$ cm^{-3}. The time for diffusion-controlled recombination in three dimensions is approximately $\{4\pi(D_{H^+} + D_{Cl^-})R_{ion}[DCl]\}^{-1} \approx 0.02$ s for $(D_{H^+} + D_{Cl^-}) = 5 \times 10^{-8}$ cm^2 s^{-1} in the bulk at 273 K and $R_{ion} = 10^{-7}$ cm. This 0.02 s recombination time is much longer than the 5×10^{-5} s pulse duration. To reduce the recombination time to 5×10^{-5} s, $(D_{H^+} + D_{Cl^-})$ must be 400 times higher in the interfacial region than in the bulk. Recombination of Cl^- and H^+ involving strictly 2-D motion requires similarly large diffusion coefficients.[57]

Acknowledgment. We are grateful to the National Science Foundation for supporting this work. We also thank Ryan Torn and Mark Wendt for measuring the surface tensions and NMR spectra of the NaOH solutions and Ilan Benjamin and Ilya Chorny for helpful discussions.

References and Notes

(1) Re, S.; Osamura, Y.; Suzuki, Y.; Schaefer, H., III. *J. Chem. Phys.* **1998**, *109*, 973.

(2) Planas, M.; Lee, C.; Novoa, J. J. *J. Phys. Chem.* **1996**, *100*, 16495.

(3) Estrin, D. A.; Kohanoff, J.; Laria, D. H.; Weht, R. O. *Chem. Phys. Lett.* **1997**, *280*, 280.

(4) Tachikawa, M.; Mori, K.; Osamura, Y. *Mol. Phys.* **1999**, *96*, 1207.

(5) Bacelo, D. E.; Binning, R. C.; Ishikawa, Y. *J. Phys. Chem. A* **1999**, *103*, 4631.

(6) Xu, S. C. *J. Chem. Phys.* **1999**, *111*, 2242.

(7) Milet, A.; Struniewicz, C.; Moszynski, R.; Wormer, P. E. S. *J. Chem. Phys.* **2001**, *115*, 349.

(8) Ando, K.; Hynes, J. T. *J. Phys. Chem. B* **1997**, *101*, 10464.

(9) Thompson, W. H.; Hynes, J. T. *J. Phys. Chem. A* **2001**, *105*, 2582.

(10) Gertner, B. J.; Hynes, J. T. *Faraday Discuss.* **1998**, *110*, 301.

(11) Bianco, R.; Gertner, B. J.; Hynes, J. T. *Ber. Bunsen-Ges. Phys. Chem.* **1998**, *102*, 518.

(12) Svanberg, M.; Pettersson, J. B. C.; Bolton, K. *J. Phys. Chem. A* **2000**, *104*, 5787.

(13) Uras, N.; Rahman, M.; Devlin, J. P. *J. Phys. Chem. B* **1998**, *102*, 93775.

(14) Devlin, J. P.; Uras, N.; Rahman, M.; Buch, V. *Isr. J. Chem.* **1999**, *39*, 261.

(15) Horn, A. B.; Chesters, M. A.; McCoustra, M. R. S.; Sodeau, J. R. *J. Chem. Soc., Faraday Trans.* **1992**, 1077.

(16) Graham, J. D.; Roberts, J. T. *J. Phys. Chem.* **1994**, *98*, 5974.

(17) Barone, S. B.; Zondlo, M. A.; Tolbert, M. A. *J. Phys. Chem. A* **1999**, *103*, 9717.

(18) Kang, H.; Shing, T.-H.; Park, S.-C.; Kim, K. I.; Han, S.-J. *J. Am. Chem. Soc.* **2001**, *122*, 9842.

(19) Baldelli, S.; Schnitzer, C.; Shultz, M. J. *J. Chem. Phys.* **1998**, *108*, 9817.

(20) Baldelli, S.; Schnitzer, C.; Shultz, M. J. *Chem. Phys. Lett.* **1999**, *302*, 157.

(21) See also Laasonen, K.; Klein, M. L. *J. Am. Chem. Soc.* **1994**, *116*, 11620 for simulations of the state of HCl in concentrated solutions.

(22) Van Doren, J. M.; Watson, L. R.; Davidovits, P.; Worsnop, D. R.; Zahniser, M. S.; Kolb, C. E. *J. Phys. Chem.* **1990**, *94*, 3265. Li, Y. Q.; Zhang, H. Z.; Davidovits, P.; Jayne, J. T.; Kolb, C. E.; Worsnop, D. R. *J. Phys. Chem. B* **2002**, *106*, 1220.

(23) Schwitzer, F.; Mirabel, P.; George, C. *J. Phys. Chem. A* **2000**, *104*, 72.

(24) Shi, Q.; Li, Y. Q.; Davidovits, P.; Jayne, J. T.; Worsnop, D. R.; Mozurkewich, M.; Kolb, C. E. *J. Phys. Chem. B* **1999**, *103*, 2417.

(25) Hanson, D. R.; Ravishankara, A. R. *J. Phys. Chem.* **1994**, *98*, 5728.

(26) Longfellow, C. A.; Imamura, T.; Ravishankara, A. R.; Hanson, D. R. *J. Phys. Chem. A* **1998**, *102*, 3323.

(27) Behr, P.; Morris, J. R.; Antman, M. D.; Ringeisen, B. R.; Splan, J. R.; Nathanson, G. M. *Geophys. Res. Lett.* **2001**, *28*, 1961.

(28) Morris, J. M.; Behr, P. M.; Antman, M. D.; Ringeisen, B. R.; Splan, J.; Nathanson, G. M. *J. Phys. Chem. A* **2000**, *104*, 6738.

(29) Miner, C. S. *Glycerol*; Reinhold Publishing Corporation: New York, 1953.

(30) Newman, A. A. *Glycerol*; CRC Press: Cleveland, 1968.

(31) Gaines, G. L. *Insoluble Monolayers at the Liquid−Gas Interface*; Interscience: New York, 1966.

(32) The surface depletion is calculated from $\Gamma = -(2RT)^{-1}(\partial\gamma/\partial \ln a_{\pm})_T$, where γ is the surface tension of the mixture and $a_{\pm} = f_{\pm}[C_3H_7O_3^-]$ is the mean ion activity of the solute. The activity coefficient $f_{\pm}$ is determined from the extended Debye−Huckel law using a dielectric constant for glycerol of 41 and an ionic radius of 5 Å. $f_{\pm}$ decreases steadily from 1 for pure glycerol to 0.46 for 0.26 M NaOH. See Hiemenz, P. C. *Principles of Colloid and Surface Chemistry*, 2nd ed.; Marcel Dekker: New York, 1986; p 395 and Aktins, P. *Physical Chemistry*, 6th ed.; Oxford University Press: New York, 1998; p 249.

(33) The TOF analysis initially assumes that DCl is present in bulk glycerol as separated Cl^- and D^+/H^+, but it may also spend a significant fraction of time as molecular DCl or as a contact-ion pair when it dissolves for only submicrosecond times (as we ultimately conclude in the Discussion section). The solutions to the diffusion equation are modeled by $p_{des}(t) = [c(x = 0, t)/c^*]^2$ for the separated ion case and $p_{des}(t) = [c(x = 0, t)/c^*]$ for the molecular or contact-ion pair cases. The p_{des} and N_{sim} distributions in Figure 1a and b for the quadratic case are similar to those for the linear case: for $\tau = 10^{-6}$ s, the peak heights of N_{sim} relative to $\tau = 0$ s are 0.935 and 0.904 for the linear and quadratic p_{des} functions, respectively. We begin the TOF analysis by assuming that DCl dissolves as separated ions because we showed in the preceding paper that DCl molecules that dissolve for longer than 10^{-2} s dissociate completely. See Figure A.1 in ref 28 for graphs of $p_{des}(t) = [c(x = 0, t)/c^*]$ at different values of τ.

(34) In employing eq 2, we ignore differences between v_{th}(HCl) and v_{th}(DCl) and any differences between β_{th}(HCl) and β_{th}(DCl).

(35) Hanson, D. R.; Ravishankara, A. R. *J. Phys. Chem.* **1993**, *97*, 12 309.

(36) Shi, Q.; Davidovits, P.; Jayne, J. T.; Worsnop, D. W.; Kolb, C. E. *J. Phys. Chem. A* **1999**, *103*, 8812.

(37) The diffusion equation can also be solved for τ values less than 10^{-6} s. However, the desorption curves for these short times may not be applicable to glycerol at 273 K. For $\tau = 10^{-7}$ s and $D = 5 \times 10^{-9}$ cm^2 s^{-1}, the average diffusion depth $(D_{HCl}\tau)^{1/2}$ is less than 3 Å, which is smaller than one glycerol molecule.

(38) Abbatt, J. P. D.; Nowak, J. B. *J. Phys. Chem. A* **1997**, *101*, 2131.

(39) Klassen, J. K.; Hu, Z. J.; Williams, L. R. *J. Geophys. Res.* **1998**, *103*, 16 197.

(40) The HCl diffusion coefficient is equal to 5×10^{-8} cm^2 s^{-1} at 294 K, where $\eta = 1300$ cP, and is estimated in the preceding paper to be 10 times smaller at 273 K, where $\eta = 12\,100$ cP.

(41) As shown in the preceding paper, K_{HCl}(294 K)/K_{HCl}(273 K) is computed to be 0.12 ± 0.02.

(42) Stern, J. H.; Nobilione, J. M. *J. Phys. Chem.* **1968**, *72*, 3937.

(43) Amdur, I.; Hammes, G. G. *Chemical Kinetics*; McGraw-Hill: New York, 1966.

(44) Torney, D. C.; McConnell, H. M. *Proc. R. Soc. London, Ser. A* **1983**, *387*, 147.

(45) Erdey-Gruz, T.; Majthenyi, L.; Nagy-Czako, I. *Acta Chim. Acad. Sci. Hung.* **1967**, *53*, 29.

(46) Agmon, N. *Isr. J. Chem.* **1999**, *39*, 493.

(47) See calculation of the diffusion coefficients of H^+ and Cl^- in the preceding paper.

(48) See ref 40 of the preceding paper.

(49) Schwartz, B. J.; King, J. C.; Harris, C. B. *Ultrafast Dynamics of Chemical Systems*; Simon, J. D., Ed.; Kluwar: Dordrecht, 1994.

(50) Benjamin, I.; Wilson, M. A.; Pohorille, A. *J. Chem. Phys.* **1994**, *100*, 6500.

(51) Buch, V. *J. Chem. Phys.* **1991**, *96*, 3814.

(52) Uras, N.; Buch, V.; Devlin, J. P. *J. Phys. Chem. B* **2000**, *104*, 9203.

(53) Isakson, M. J.; Sitz, G. O. *J. Phys. Chem. A* **1999**, *103*, 2044.

(54) The overall rate for DCl dissolution, DCl dissociation, H^+ and Cl^- recombination, and HCl evaporation scales as F_{inc}^2 at early times ($t < t_{pulse} = 50$ μs) and as F_{inc} at steady state ($t \gg t_{pulse}$).

(55) Bauer, S. H. *Annu. Rev. Phys. Chem.* **1979**, *30*, 271.

(56) Recent results by Li et al. (ref 22) show that the mass accommodation coefficients in ethylene glycol at 303 K are 0.37 for HCl (intermediate between the water and glycerol values) and 0.96 for HBr (close to the glycerol value).

(57) For strictly 2D ion−ion recombination, as might occur on the surface of glycerol, the recombination rate is approximately given by $k_{2D} = (D_{H^+} + D_{Cl^-})[ion]_{surf}$. If $k_{2D} = 1/(5 \times 10^{-5}$ s) and $[ion]_{surf} = 0.07F_{inc}t_{meas}$, then $[ion]_{surf} = 4 \times 10^8$ cm^{-2} for $F_{inc} = 1 \times 10^{14}$ cm^{-2} s^{-1}, and $t_{meas} = 5 \times 10^{-5}$ s. In this case, $(D_{H^+} + D_{Cl^-})$ must be at least 5×10^{-5} cm^2 s^{-1}, which is 1000 times larger than the bulk value of 5×10^{-8} cm^2 s^{-1}.